



CGMS-36 EUM-WP-24
v1, 19 September 2008
Prepared by EUMETSAT
Agenda Item: II/5
Discussed in WGII

POLAR CAP WINDS AVHRR FROM AVHRR ONBOARD METOP-A

Data from the 11 μm channel of the imaging radiometer AVHRR/3 (Advanced Very High Resolution Radiometer) onboard Metop-A are used to derive winds over the polar areas. The algorithm has been developed at CIMSS (Cooperative Institute for Meteorological Satellite Studies) and evaluates cloud motions which are derived from overlapping areas of subsequent orbits. The original code has been modified with respect to image navigation and mapping and is capable to ingest either EPS (EUMETSAT Polar System) Level 0 or Level 1B data. Moreover, cloud top pressures extracted from co-located IASI (Infrared Atmospheric Sounding Interferometer) measurements serve as additional information to validate the height assignment of the retrieved winds. For both, Arctic and Antarctic regions, the assigned altitudes show the strongest correlation between 300 hPa and 700 hPa.

After successfully finishing the prototyping, the prime focus will be on the validation of the results, the generation of a reference test data set and the definition of the algorithm requirements and the product format for EUMETSAT's EPS Ground Segment.

Polar Cap Winds AVHRR from AVHRR onboard Metop-A

Jörg Ackermann, Dieter Klaes, Peter Schlüssel

EUMETSAT, Am Kavalleriesand 31, D-64295 Darmstadt, Germany

1 INTRODUCTION

The first polar-orbiting European meteorological satellite Metop-A carries the six-channel imaging instrument AVHRR/3 (Advanced Very High Resolution Radiometer), which is already flown onboard the United States' NOAA (National Oceanic and Atmospheric Administration) K, L, M, N weather satellites (Klaes et al., 2007). At present, AVHRR/3 data are routinely used for e.g. cloud detection, monitoring of sea ice, snow coverage and vegetation, and the determination of surface temperature and reflectance. More recent applications comprise the derivation of winds from AVHRR/3 data using the overlapping swaths of images from subsequent orbits in the polar areas. These tracking algorithms for deriving wind vectors have been originally developed for geostationary satellite data (Schmetz et al., 1993) and were later adapted to process data from the Moderate Resolution Imaging Spectroradiometer MODIS onboard NASA's polar orbiting satellites Terra and Aqua (Key et al., 2003). Since the SWG (Science Working Group) has expressed a strong interest of the user community to receive polar cap winds derived from AVHRR/3 onboard Metop-A operationally, activities have been kicked off at EUMETSAT with the objective to make a polar wind product available at the end of 2008. To scientifically support the development of a corresponding product processing facility within the EPS Ground Segment, the winds algorithm from CIMSS is used for prototyping activities and validation purposes. In addition, it is envisaged to extend the height assignment of retrieved wind vectors towards using co-located cloud top pressures derived from IASI measurements.

It is the scope of this note to briefly discuss the current status of the prototyping activities at EUMETSAT using the winds algorithm from CIMSS. Finally, potential future activities related to the derivation of polar cap winds are sketched.

2 MAIN TEXT

METHOD

The core of the winds algorithm is taken over from the code made available by CIMSS. Extensions have been made with regard to the format of the input data, the mapping of the data sets, and the inclusion of coincident IASI Level 2 data. It should be noted that there is no explicit cloud detection algorithm applied to the AVHRR/3 data prior to the selection of potential targets to be used for the derivation of the atmospheric motion winds (AMV). Instead, several cluster analysis techniques are applied directly to brightness temperatures calculated from the Earth view radiances.

Input Data

The following input data are used for the wind derivation:

Three subsequent orbits of AVHRR/3 Level 1B data in EPS format: these data sets already contain geolocated radiances. The pre-processor selects the 6000 scan lines closest to the poles, extracts the corresponding channel 4 radiances and converts them into brightness temperatures. Geolocation information of an individual scan line in the original data sets is available for each 20th pixel only. Using these tie-points, the data are interpolated to get geographical latitudes and longitudes for each pixel. The interpolation algorithm takes into account the discontinuities at the dateline and the singularities at the poles (see Appendix for further details).

The forecast data sets in GRIB have a resolution of 1° in both latitude and longitude direction. They comprise vertical profiles of atmospheric temperatures and wind components at the following pressure levels: 1000 hPa, 850 hPa, 700 hPa, 500 hPa, 400 hPa, 300 hPa, 250 hPa, 200 hPa, 150 hPa, 100 hPa. For the temperature profiles, the values at the surface, and at 70 hPa and 50 hPa are used, too. All forecasted data sets should be within a time range of nine hours of the satellite data.

Alternatively, the processor is capable to use AVHRR/3 raw (Level 0) data and actual orbital elements as input. In connection with an instrument calibration algorithm, geolocated channel 4 brightness temperatures are generated for each pixel.

In the current version of the code, the brightness temperatures are converted into 8-bit counts using a pre-defined look-up table. This loss of accuracy should not have a negative impact on the winds retrieval from the AVHRR/3 using channel 4 measurements alone.

Geolocation Accuracy

Apart of the lack of a water vapour channel, it is often mentioned that compared to MODIS, two main drawbacks of AVHRR/3 are low spatial resolution and inaccurate pixel geolocation. AVHRR/3 onboard Metop-A alleviates the latter two shortcomings, since the measurement data are globally available with 1.1 km resolution near nadir and since the instrument's time stamps exhibit no clock error, which has been the main cause for along-track errors of geolocation in the past. Because the polar cap winds algorithm relies on a sequence of images which show a distinct target under different viewing angles, accurate geolocation is an essential prerequisite for the operational use of winds retrieved from this imagery. Thus, the prototype includes an automated procedure which checks the actual pixel geolocation against the true coastlines using Normalized Difference Vegetation Index (NDVI), channels 2 reflectances, channel 4 brightness temperatures, or brightness temperature differences between channel 4 and 5. Figure 1 displays the typical geolocation accuracy of ± 1 pixel for AVHRR/3 onboard Metop-A.

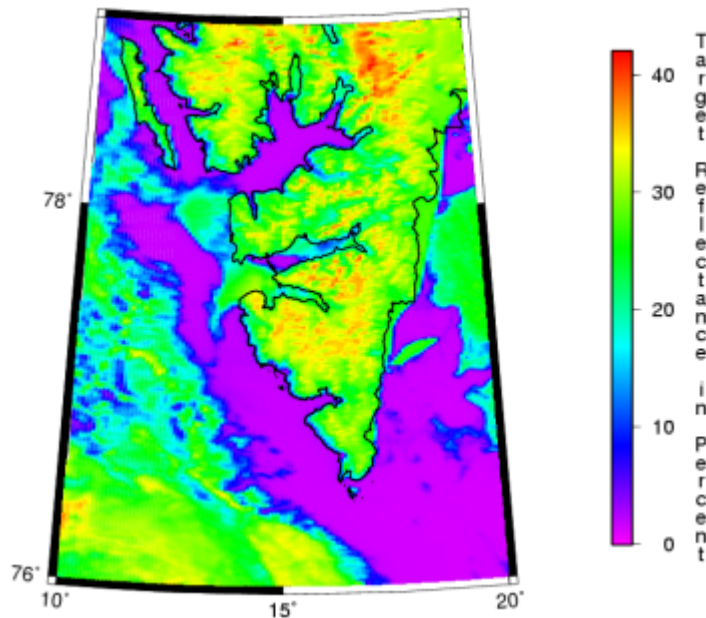


Figure 1: Typical Geolocation of Metop-A AVHRR/3 by visual inspection of channel 2 target reflectance in the Svalbard area (4. June 2008, 8:32 UTC). For cloud- and ice-free conditions, the match between the expected and the true coastline is in the range of 1 pixel. This accuracy has been achieved by reducing the maximum scanning angle to 55.2° and by applying the following attitude corrections: pitch 0.117°, roll -0.125°, yaw -0.034°

Mapping

In contrast to geostationary data processing, even a fixed target monitored during subsequent overpasses of one or several polar orbiting satellites is sampled under different viewing angles. Therefore, proper tracking of features seen under different viewing angles requires the mapping of data onto a common projection. This processing step can consume a lot of CPU time especially for cases, where the regular grid in the mapped projection has a higher resolution than the imager data to be mapped. The CIMSS algorithm requires the mapping of the original data onto a polar stereographic grid with 2800 lines and 2800 elements roughly covering the zone poleward from $\pm 60^\circ$ latitude. This corresponds to a resolution of about 2 x 2 km, which is coarser than the resolution of the original data near nadir (1.1 km). When approaching towards the scan edges however, the pixel extension increases to 6.2 x 2.3 km, while subsequent scan lines tend to overlap. As a result, a standard nearest neighbour mapping would show some gaps in the mapped data when approaching the scan edges. Evidently, for those areas, a target selection to derive winds would be erroneous. Therefore, a new algorithm has been developed which is especially adapted to AVHRR/3 scanning properties and provides full coverage of the projected data at the swath edges.

Target Selection and Initial Height Assignment

From a triplet of three subsequent scenes separated by about 100 minutes, the middle image is used for the target selection. A target box with an extension of 13 x 13 pixels in the polar stereographic domain is successively shifted through the whole image. Using local bidirectional gradients of brightness counts, targets are considered as suited for tracking, if they show a high spatial variability (threshold: 7 counts/pixel)

in combination with a local minimum of brightness temperatures. Physically, those targets should represent the edges of optically thick clouds.

For each selected target, an initial height assignment is performed using the nearest forecast temperature profiles interpolated to the geographical position of the target. Histograms are computed from the brightness counts within the target box. The cloud top temperature is derived from the brightness temperature, which corresponds to the coldest 5% of the pixels. Evaluation of higher-order cumulants is performed by expanding the probability distribution function of the histogram into a series of functions with known mathematical properties. This allows the identification of several modes in the histogram, which are attributed to the clouds and the surface, respectively. The distance between the cloud top and the cloud mode is then used to determine the cloud base temperature and hence, the cloud base pressure. The cloud base pressure is important, when scattered cumulus clouds are used as tracers, because the motion of their bases is more characteristic for the atmospheric wind than the displacement of their cloud tops. If the forecasted temperature profile shows an inversion, the cloud base pressure is not determined. If, for a distinct target, a meaningful cloud base pressure could be determined, it is given the preference above the corresponding cloud top pressure value.

Target Tracking

All selected targets with initial height assignment are considered for tracking. A search area with an extension of 49X49 pixels in the polar stereographic image is created for each target area. A wind vector from the forecast data set is interpolated to the position of the target. According to this forecasted wind speed and direction, the centres of the search boxes in the images of the subsequent and the previous orbits, respectively, are computed. Once the centres have been determined, the original target is shifted within these two search boxes and the correlations for the co-located pixel pairs are computed for each displacement. The shifts, which correspond to the best correlations between the target area and the two search areas, give two wind vectors, one estimate for the atmospheric motion between the scene of the previous orbit and the target image, and one for the motion between the scene of the target image and the subsequent orbit.

Quality Checks

Acceleration checks are performed for both AMV's retrieved for one target box, and the averaged vector is compared against and the interpolated wind from the forecast profile. If either the retrieved U- or V-components differ by more than 10 m/s from the forecast, a corresponding flag is set.

Furthermore, there is a two-step procedure for deriving individual series of quality indicators for each retrieved wind vector: the first step includes a series of consistency checks of an actually retrieved wind vector with surrounding AMV's (Holmlund, 1998). The individual tests rely mainly on the following criteria:

1. Differences in direction for the same location, but subsequent image pairs
2. Differences in velocity for the same location, but subsequent image pairs
3. Differences in individual wind components for the same location, but subsequent image pairs
4. Differences in the retrieved vs, forecasted wind vector for the same location

5. Differences in neighbouring retrieved wind vectors for the same image pairs (only performed in a predefined pressure range of 50 hPa)

The result of this test sequence is a normalized quality indicator for each wind vector, which does not reject an individual vector, but has a lower value for inaccurate or biased AMV's.

The second step of the test procedure relies on a three-dimensional objective analysis of the retrieved winds using the forecasted wind and temperature profiles (Hayden and Pursor, 1995): as a pre-processing step, weighted gross error limit checks are performed using the differences between the forecasted and the retrieved wind components and the related temperature and pressure values. By minimizing a so-called penalty function for each measurement, the derived height assignments are adjusted. This penalty function is computed for each wind vector and each forecast pressure level (see the section Input Data). It sums up all weighted and squared differences for the horizontal dimension of the forecast fields, which have passed the above mentioned gross error limit checks. Together with a maximum allowed value of the penalty function, a further quality indicator is derived.

3 CONCLUSIONS

RESULTS

The described winds algorithm has been applied to a triplet of Metop-A AVHRR/3 data from 4. June 2008. From three subsequent orbits, data located over the Arctic and Antarctica have been selected and remapped onto a polar stereographic projection. To illustrate the coverage of three subsequent scenes, data from all three overpasses are plotted on one sheet (Figure 2). Winds vectors are retrieved for a rhomboid-shaped area, which is probed during each overpass of the satellite. Different colours of the wind vectors are related to different intervals of the height assignments.

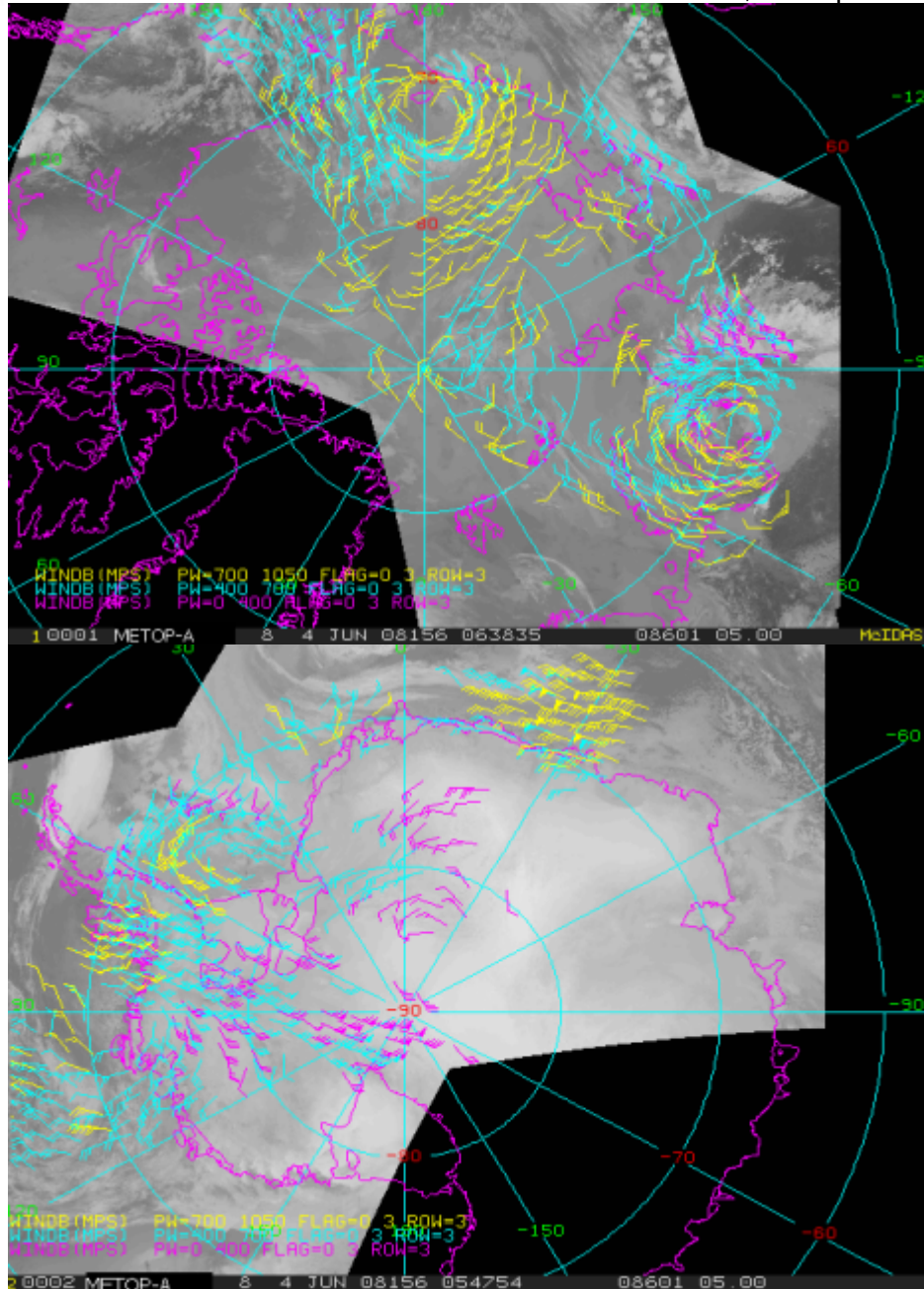


Figure 2: Retrieved polar cap winds for the Arctic (upper part) and Antarctic (lower part) for June 4, 2008. Different colours of the bars illustrate three different height intervals; yellow: from surface to 700 hPa; blue: from 700 hPa to 400 hPa; magenta above 400 hPa. The starting times for the target images are 6:38:35 UTC for the Arctic and 5:47:54 for the Antarctic, respectively. For displaying the data, the McIDAS software has been used.

As it was already previously mentioned, a possible extension of the current winds algorithm for Metop-A data is the use of co-located IASI data for the height assignment of the wind vectors. To judge on the potential impact of IASI derived cloud top pressures onto the original height assignment, from the IASI Level 2 data processed in the EPS Ground Segment the following pixels have been selected:

- The IASI pixel is closer than 10 km to a retrieved wind vector
- There is only one detected cloud layer
- The percentage of clear sky within the IASI pixel may not exceed 20%

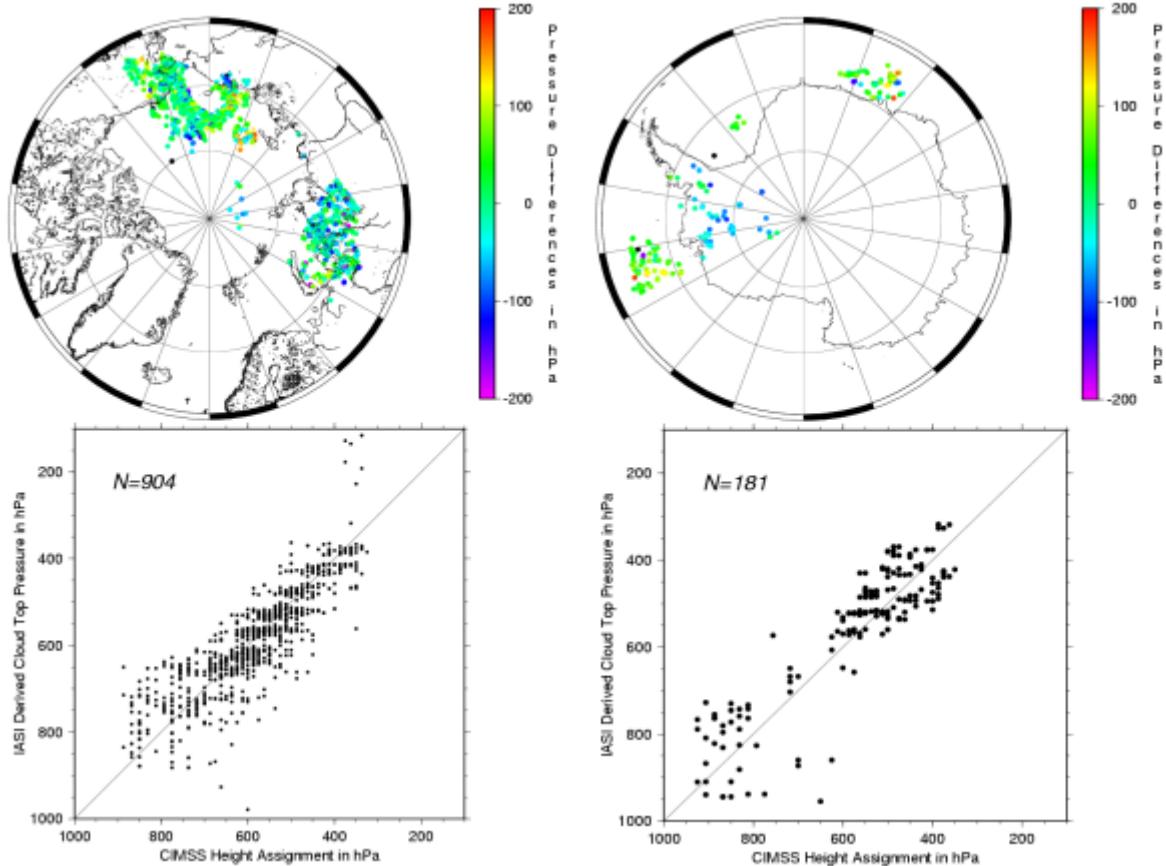


Figure 3: Comparison between wind height assignment retrieved from the CIMSS code and the co-located cloud top pressure from the IASI Level 2 product for the Arctic (left) and the Antarctic (right)

For each of the IASI pixel which meets the above mentioned criteria, the cloud top pressure value is compared against the assigned wind height retrieved from AVHRR/3 channel 4 data and forecasted temperature profiles. The results for both polar caps are plotted in Figure 3. Evidently, the highest correlations exist between 300 hPa and 700 hPa, whereas a weaker dependence is retrieved for lower altitudes. Since there is no significant bias, the larger scattering of the data pairs will most likely not have a single cause. Further investigations are needed to resolve this issue.

OUTLOOK

The prime goal is to have a validated algorithm for the operational processing of polar cap winds from AVHRR/3 onboard Metop-A implemented into the EPS Ground Segment in due time. Apart of new features like the inclusion of co-located IASI derived cloud top pressures, it is also important to make use of potential heritages from already existing operational winds code for the evaluation of data from geostationary satellites. Therefore, the algorithm presented here will not necessarily have the same architecture as the future operational processor. It will, however, serve as the baseline for the validation of the operational processor, since it reflects the actual state-of-art with respect to the generation of winds from polar orbiting satellites.

REFERENCES

Hayden, C.M., and R.J.Pursor, 1995: Recursive filter objective analysis of meteorological fields: applications to NESDIS operational processing, *J. Appl. Meteorol.*, **34**, pp 3-15.

Holmlund, K., 1998: The utilization of statistical properties of satellite derived atmospheric motion vectors to derive quality indicators, *Wea. Forecasting*, **12**, pp 1093-1103.

Key, J., D. Santek, C.S. Velden, N. Bormann, J.-N. Thepaut, L.P. Riishojgaard, Y. Zhu, and W.P. Menzel, 2003: Cloud-drift and water vapour winds in the polar regions from MODIS, *IEEE Trans. Geosci. Remote Sens.*, **41(2)**, pp 482-492.

Klaes, K.D., M. Cohen, Y. Buhler, P. Schlüssel, R. Munro, J.-P. Luntama, A. von Engeln, E. Ó Cléirigh, H. Bonekamp, J. Ackermann, and J. Schmetz, 2007: An introduction to the EUMETSAT Polar System, *Bull. Amer. Meteor. Soc.*, **88**, 7, pp 1085-1096.

Schmetz, J., K. Holmlund, J. Hoffman, B. Strauss, B. Mason, V. Gaertner, A. Koch, and L. van de Berg, 1993: Operational cloud motion winds from METEOSAT infrared images, *J. Appl. Meteorol.*, **32**, pp 1206-1225.

APPENDIX

In the following, an algorithm is described, which allows to assign the geolocation of each AVHRR pixel from the tie-points. For most cases, a linear interpolation is sufficiently accurate. However, the interpolation at the dateline and near the geographical poles is more complex and has to be treated separately.

Standard Linear Interpolation

Let λ and ϕ denote the geographical longitude and latitude of an arbitrary point at the Earth's surface, respectively. The range of λ is from -180° to $+180^\circ$, and ϕ can have values between -90° (South Pole) and 90° (North Pole). Furthermore, the total number of tie-points per scan line is denoted with N and the distance between two subsequent tie-points is Δ pixels. Thus, for each scan line, there exists geolocation information for $\lambda_1, \lambda_2, \dots, \lambda_N$ and $\phi_1, \phi_2, \dots, \phi_N$ with $N = 51$ or $N=103$. The numbering of the tie-points is in scanning direction, i.e. from the right to the left when looking into the flight direction of the satellite.

The objective is to retrieve the geolocation information for each pixel k , i.e. for

$\lambda_1, \lambda_2, \dots, \lambda_K$ and $\phi_1, \phi_2, \dots, \phi_K$ with $K = 409$ or $K= 2048$. If the pixel number of the first tie-point is denoted with k_{start} (i.e., $k_{start} = 5$ or $k_{start} = 25$), the range of k for interpolation is:

$$k_{start} \leq k \leq (N - 1) \Delta + k_{start} + 1$$

The following numerical equation determines the indices of the two tie-points n and $n+1$, which are closest to a pixel k :

$$n = \text{int} \left(\frac{k - k_{start}}{N} \right) + 1$$

Once n is determined, the interpolated values for the geolocation of the corresponding pixel k are:

$$k = n + i \frac{k - k_{start}}{N} \quad \text{with: } i = k - k_{start} - (n - 1)N \quad \text{and} \quad n + 1 = n$$

$$k = n + i \frac{k - k_{start}}{N} \quad \text{with: } i = k - k_{start} - (n - 1)N \quad \text{and} \quad n + 1 = n$$

If values have to be extrapolated at the scan edges, the equations above are valid, when n is set to 1 for $k = 1, \dots, k_{start} - 1$ (right scan edge) and n is set to N for $k = k_{start} + (N - 1)N, \dots, K$ (left scan edge). The formula discussed above work for most of the cases. However, due to the discontinuity of the geographical longitude at the date line and due to the singularities at the geographical poles, the interpolation scheme has to be modified for these two cases or combinations of them. The algorithm to handle those cases is discussed below.

Interpolation at the Dateline

If the dateline is located between two subsequent tie-points, a linear interpolation is only possible for the geographical latitude. For the geographical longitude, however, the determination of $n + 1 = n$ leads to erroneous results. To overcome this, the rules for the linear interpolation have to be modified.

In the first step, the occurrence of the dateline between two tie-points $n + 1$ and n is identified:

$$|n + 1| - |n| = 180$$

The validity of this expression ensures that the Greenwich meridian is excluded. In addition, one of the following conditions is necessary:

$$n = 0 \quad n + 1 = 0 \quad \text{(Case A)}$$

$$n = 0 \quad n + 1 = 0 \quad \text{(Case B)}$$

Depending on the selected case, θ_k is calculated via:

$$\theta_k = \frac{360}{n-1} (k-1) + \theta_1 \quad (\text{Case A})$$

$$\theta_k = \theta_1 + \frac{360}{n-1} (k-1) \quad (\text{Case B})$$

These values of θ_k have to be implemented into the corresponding equations for the standard linear interpolation. Then, the retrieved values for θ_k have to be checked whether they are still within the expected range of -180° to $+180^\circ$. If the actual value of θ_k is less than -180° , a value of 360° has to be added to get the final θ_k , if the actual value is greater than 180° , a value of 360° has to be subtracted from θ_k . Note that a potential correction for the impact of the dateline has to be performed before the standard interpolation and the interpolation at the poles, which is described hereafter.

Interpolation at the Poles

Due to the increasing curvature of the latitude belts, a linear interpolation of the geographical position for a distinct pixel breaks down in the poleward regions. Therefore, an algorithm has been developed which allows an accurate interpolation of the pixel geolocation from a given set of tie-points near the poles. It is described below and illustrated in Figure 4.

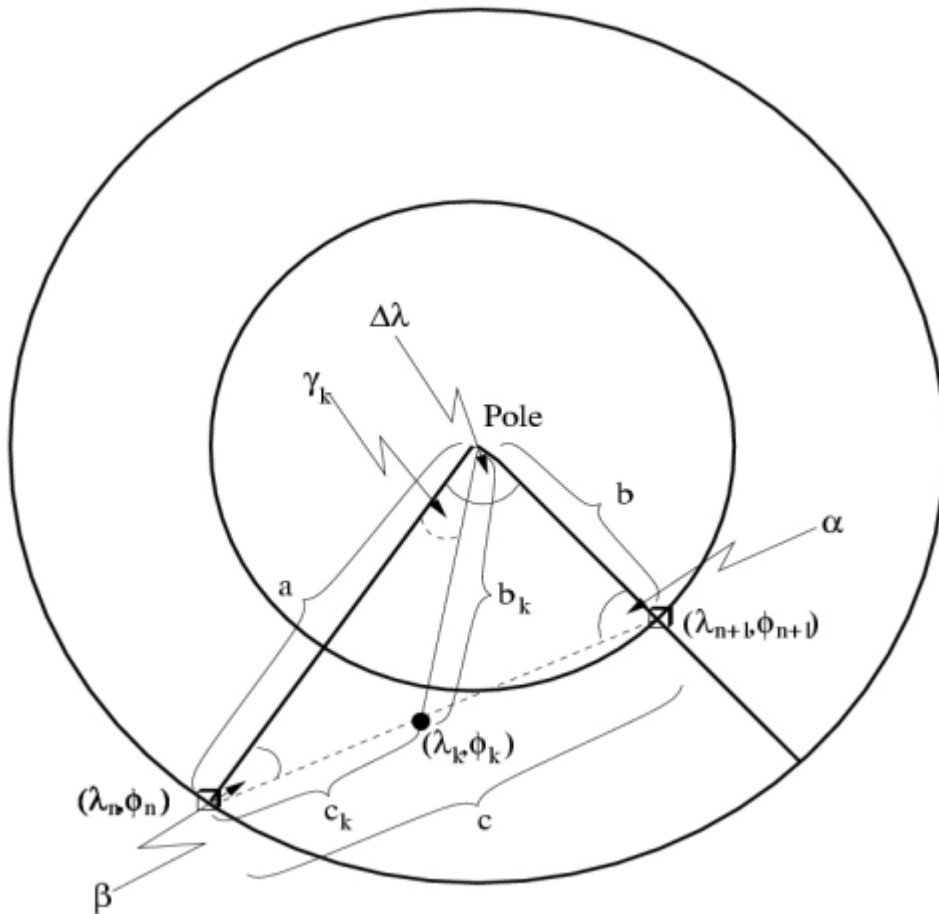


Figure 4: Principle of the geolocation interpolation near the pole. The pole is in the center, the latitudes are given as circles, and the longitudes as straight lines.

Extensive testing revealed that the interpolation at the poles should be applied, when the absolute of the geographical latitude for both tie points is larger or equal 87° , i.e. the following formulas are a prerequisite for this special case:

$$\begin{aligned} | \phi_n | &\geq 87 \\ | \phi_{n+1} | &\geq 87 \end{aligned}$$

Referring to Figure 4, the values for a and b are:

$$\begin{aligned} a &= 90 - | \phi_n | \\ b &= 90 - | \phi_{n+1} | \end{aligned}$$

With $\phi_{n+1} = \phi_n + \Delta\phi$, the cosine law allows the determination of c:

$$c = \sqrt{a^2 + b^2 - 2ab \cos(\gamma_k)}$$

Thus, the remaining angles of the triangle (Tie-point n+1, Pole, Tie-point n) are:

$$a \cos \frac{b^2 + c^2 - a^2}{2bc}$$

180 | |

The knowledge of is necessary to compute the sides and angles of a triangle (Interpolated Geolocation, Pole, Tie-point n). For a given side c_k (see Figure 4), application of the cosine law gives:

$$b_k = \sqrt{a^2 + c_k^2 - 2ac_k \cos(\)}, \text{ whereas}$$

$$c_k = i \frac{c}{N} \text{ with: } i = k - k_{start} \quad (n - 1) \quad N$$

Depending on the sign of , the angle k , which is closely related to the desired value of k , is:

$$k = a \cos \frac{a^2 + b_k^2 - c_k^2}{2ab_k} \quad \text{for } 0$$

$$k = a \cos \frac{a^2 + b_k^2 - c_k^2}{2ab_k} \quad \text{for } 0$$

If the dateline is between the two tie-points $n - 1$ and n (either Case A or Case B), the sign of the retrieved k has to be inverted. Finally, the interpolated latitude and longitude are given as:

$$k = n - k \quad \text{for the Northern Hemisphere}$$

$$k = b_k - 90 \quad \text{for the Southern Hemisphere}$$